Measurements of electron emission under electron impact on BN sample for incident electron energy between 10eV and 1000eV

M. Villemant, Mohamed Belhaj, Pierre Sarrailh, Sarah Dadouch, Laurent Garrigues, C. Boniface

Measurements of electron emission under electron impact on BN sample for incident electron energy between 10 eV and 1000 eV

M. Villemant[1], M. Belhaj[1], P. Sarrailh[1] S. Dadouch[1], L. Garrigues[2] and C. Boniface[3]

[1] *ONERA/DPHY, Université de Toulouse F-31055 Toulouse – France*
[2] *LAPLACE, Université de Toulouse, CNRS, Toulouse, France*
[3] *Propulsion, Pyrotechnics and Aerothermodynamics section, CNES - French National Space Agency, 18 Avenue Edouard Belin, F-31401 Toulouse, FRANCE*

*** Missing PACS ***

Abstract –Electron emission measurements have been performed on a BN sample by using a new specific protocol and experimental set-up, which allows characterizing electron emission under electron impact on resistive material in a short time and with a wide variety of extracted data: total electron emission yield, emitted electron energy distribution, elastically backscattered electron emission yield and energy efficiency of electron-surface interaction. Methodology, calibration, biases corrections and results are presented in this letter. Results are compared to that measured on another material SiO_2. As there are few published data on electron emission at low incident electron energy on BN sample, it is expected that these measurements could be useful for numerous studies implying electron emission on BN surface.

The electron emission characteristics at low incident electron energy (few hundreds of eV and lower) are scarce. Nevertheless, the knowledge of electron emission at low energy is highly needed for several applications. In space industry, electron emission impacts Hall Thrusters plasma behavior used for satellites attitude control and orbit rising [1, 2] which could be critical due to the emitted electrons transit from one wall to another leading to a resonance phenomenon [3]. Besides, dielectrics materials — and specifically BN–SiO_2 and BN — are massively used for Hall thrusters channel wall [1, 2, 4]. In this context, electron emission is also critical for the design and manufacturing of satellites RF components such as wave-guides [5] and ceramics are also used in these components [6, 7]. Besides, electron emission has also an incidence on other applications such as particles accelerators [8, 9], fusion reactor functioning (in particular near divertors) [10] or for dusty plasma modelling in fusion reactors or space [11–13]. For these reasons during the last decades a renewed interest has been shown for electron emission especially at low energy [14] and on dielectrics [15].

However electron emission measurements are complex on ceramics due to the charging effects [15]. A method of electron emission measurement on dielectrics, which essentially relies on the use of tens of nanometers thin samples, was used and measurements results are presented in this letter. This method frees up the measurement process from ceramics high resistivity and allows thus carrying out these measurements. Electron emission measurements were performed on a thin BN layer deposited on a copper substrate by plasma sputtering. Five characteristic values of electron emission are extracted from measurements on the BN samples and are presented in this letter: the total electron emission yield, the elastically backscattered electron emission yield, the emitted electron energy distribution and the energy efficiencies of electron-wall interaction for monoenergetic incident electron beam (R_{E}) and Lambertian distribution of incident electrons (R_{T}).

Electron emission is the result of three phenomena: secondary electron emission, elastic backscattering and inelastic backscattering. Secondary electron emission is the ejection of electron due to ionization process under the impact of incident electrons. Most of the secondary electrons are emitted in the vacuum with an energy of a few eV. Elastic backscattering is the reemission of incident electrons which only endured elastic collisions in the material. They reemerge in the vacuum with an energy equal to the incident energy (E_0). Inelastic backscattering is

the re-emission in the vacuum of incident electrons which encountered at least one inelastic collisions in the material. They reemerged in the vacuum with an energy lower than E_0. The secondary electron emission yield (noted δ) is the ratio of the emitted secondary electron flux (Γ_{se} [$m^{-2}\,s^{-1}$]) on the incident electron flux (Γ_0 [$m^{-2}\,s^{-1}$]). Elastically backscattered electron emission yield (noted η_e) is the flux of elastically backscattered electrons (Γ_{eb} [$m^{-2}\,s^{-1}$]) on the incident electron flux. Finally, the inelastically backscattered electron yield (noted η_i) is the flux of inelastically backscattered electron (Γ_{ib} [$m^{-2}\,s^{-1}$]) on the incident electron flux.

$$\delta = \frac{\Gamma_{se}}{\Gamma_0} \qquad \eta_e = \frac{\Gamma_{eb}}{\Gamma_0} \qquad \eta_i = \frac{\Gamma_{ib}}{\Gamma_0} \tag{1}$$

The sum of these three terms is the total electron emission yield (noted σ):

$$\sigma = \frac{\Gamma_e}{\Gamma_0} = \frac{\Gamma_{se} + \Gamma_{eb} + \Gamma_{ib}}{\Gamma_0} = \delta + \eta_e + \eta_i \tag{2}$$

In eq.(2), Γ_e [$m^{-2}\,s^{-1}$] is the total emitted electron flux. The emitted electron energy distribution is defined as the normalized derivative of emitted electron flux with respect to the emitted electron energy:

$$\delta_E\Gamma_e = \frac{1}{\Gamma_e}\frac{d\Gamma_e}{dE} \tag{3}$$

Measurements have been carried out at very low incident electron energy (between 10 eV and 1000 eV), and at room temperature on an ultra-high-vacuum experimental set-up specially designed for electron emission measurement at low energy. As electron emission depends essentially on the material properties on the first tens of nanometers of the sample, it is essential to ensure the sample cleanliness. To do so, the BN samples were eroded with an ion gun before measurement and the samples surface cleanliness has been controlled by Auger Electron Spectroscopy and X-ray photo-electron spectroscopy.

Total electron emission yield measurement protocol exposed in [16] consists in measuring incident electron current and emitted electron current. The total electron emission yield is then deduced according to the current conservation law. Elastically backscattered electron emission yield data can be deduced experimentally from the emitted electron energy distribution and total electron emission yield measurements as shown in [17]. Indeed, as the emitted electron energy distribution data are normalized, the proportion of elastically backscattered electrons on the total number of electrons is equal to the integral of the emitted electron energy distribution under the elastically backscattered electrons peak (cf. colored area on Fig.1). The elastically backscattered electron emission yield value can then be obtained by multiplying this value by the total electron emission yield:

$$\eta_e(E_0) = \sigma(E_0)\int_{E_{e,inf}}^{E_{e,sup}} \delta_E\Gamma_e(E, E_0).dE \tag{4}$$

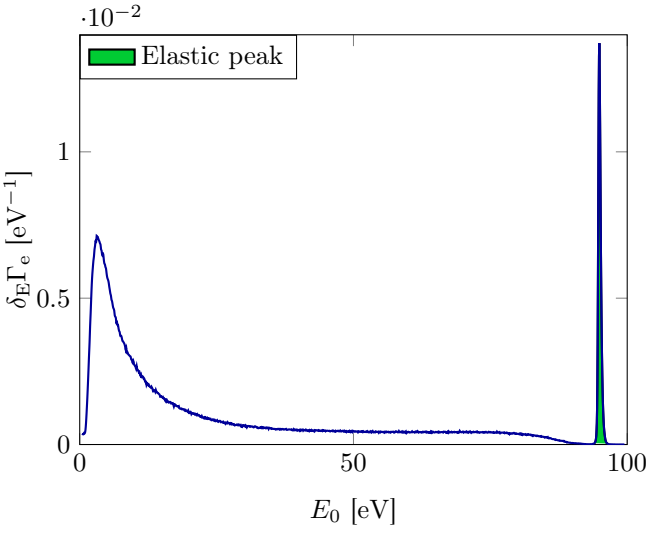

Fig. 1: EEED of BN sample irradiated with $E_0 = 90$ eV. The area under elastically backscattered electrons peak (used for EBEEY calculation) is higlighted

In eq.(4), $E_{e,inf}$[eV] is the energy at the beginning of the elastic peak and $E_{e,sup}$ [eV] the energy at the end of the elastic peak. Emitted electron energy distribution measurements are very sensitive and need to be calibrated as it has been shown in [18].

Energy efficiency of electron-wall interaction (R_E) is the ratio of the total kinetic energy of the emitted electrons during electron emission on the total kinetic energy of the incident electrons to the wall. R_E measurement methodology and calibration are described in [18].

$$R_E(E_0) = \frac{\Gamma_e\,\langle E_e\rangle}{\Gamma_0 E_0} = \sigma(E_0)\frac{\langle E_e\rangle}{E_0} \tag{5}$$

With $\langle E_e\rangle$ [eV] the mean energy of the emitted electrons. R_E is measured on BN sample for a monoenergetic incident electron flux.

Samples charging is usually the major obstacle to electron emission measurements on dielectric material. In order to prevent it, electron emission measurements have been carried out on samples with a thickness below 100 nm. This method is only applicable for electron emission measurements at very low E_0 ($E_0 < 1000$ eV) so that incident electrons penetration depth remains below a dozen of nanometers [19, 20]. The samples were produced using a method described in [21]. Fig.2 shows the BN sample charging relatively to the imposed sample holder potential bias (φ) by the incident electron flux, that is, the total surface potential minus the bias ($V_{acc} = -20$ V). It can be observed that, thanks to their very low thickness, φ is saturated to a few volts (φ between -2.7 V and 2.5 V, cf. Fig.2) and that total surface potential always remains negative preventing any emitted electrons recollection. On the electron emission measurements, residual charging bias is corrected by using the emitted electron

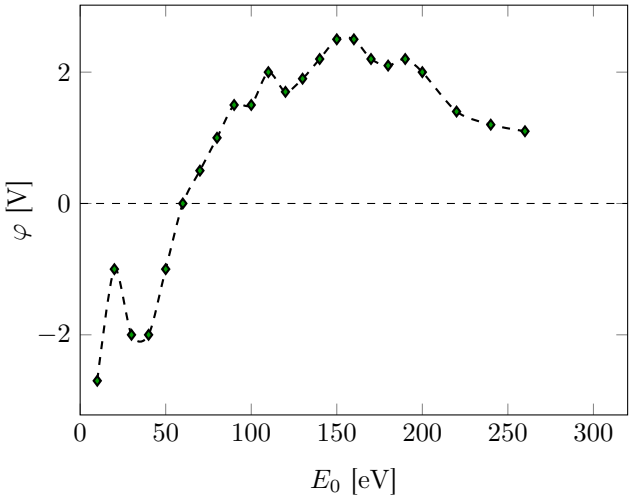

Fig. 2: Surface charging of BN sample depending on the incident energy E_0 measured from EEED offset

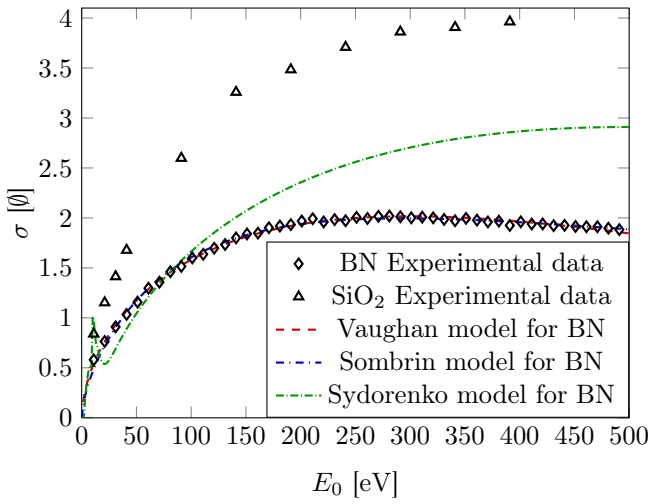

Fig. 3: Total Electron Emission Yield of BN and SiO_2 samples

energy distribution measurements as described in [18].

Total electron emission yield measurements are presented on Fig.3 as a function of the incident electron energy E_0. Several values of interest can be noticed on this figure. First of all, it can be observed that the first point of crossover of BN is reached for $E_0 = 37\,\text{eV}$ and that the maximum of total electron emission yield is equal to $\sigma_{\max} = 2.19$ at $E_0 = E_{\max} = 281\,\text{eV}$. BN total electron emission yield has been compared to SiO_2. It can be observed that total electron emission yield is twice lower on BN than on SiO_2. Measurements have been fitted with Vaughan's [22] and Sombrin's [5] models. For both models, parameters and correlation coefficient are summarized in Table.1. It can be seen that both fitted models are in good agreement with experimental data. On this figure, total electron emission yield model presented by Sydorenko in his Ph.D. [23] and that has been used in several articles [24, 25].

Fig.4 shows a comparison between total electron emission yield values measured during this work and values of total electron emission yield measured by Dunaevsky et al. [26] and by Bugeat et al. [26]. It can be observed that there is a good correlation between experimental values that have been measured here and the ones measured by Dunaevsky et al. Nonetheless this paper allows extending available data about electron emission on BN. Indeed this work shows original values of electron emission on BN such as total electron emission yield as a function of incident electron energy and for several incident electron angle (cf. Fig.8 and 9), elastically backscattered electron emission yield (cf. Fig.5), energy efficiency of electron-wall interaction for a monoenergetic incident electron flux (cf. Fig.6) and for Lambertian distribution of incident electrons (cf. Fig.7).

Fig.8 and 9 show the measurements of total electron emission yield as a function of incident electron energy and for several incident electron angle. It can be observed that the total electron emission yield increases with incident electron angle to the surface normal. These experimental data can be fitted with Vaughan fitting formula [22]:

$$\sigma(E_0,\theta_0) = \sigma_{\max}(E_0,\theta_0)\left[v(E_0,\theta_0)\exp(1-v(E_0,\theta_0))\right]^k \quad (6)$$

$$v(E_0,\theta_0) = \frac{E_0}{E_{0,\max}(\theta_0)} \quad (7)$$

$$E_{0,\max}(\theta_0) = E_{0,\max}(\theta_0=0)\left(1+\frac{k_s}{\pi}\theta_0^2\right) \quad (8)$$

$$\sigma_{\max}(\theta_0) = \sigma_{\max}(\theta_0=0)\left(1+\frac{k_s}{2\pi}\theta_0^2\right) \quad (9)$$

Where $E_{0,\max}(\theta_0 = 0)$, $\sigma_{\max}(\theta_0 = 0)$ and k are given in Table 1 and k_s has been taken equal to 1. Figure 9 shows good correlation between experimental data and Vaughan model for incident electron energy lower than 200 eV. This set of measurements has not yet been published and presents interest for electron emission modelling as it is common that incident electrons hit the material surface with an incident angle other than normal to the surface.

Elastically backscattered electron emission yield of BN is represented on Fig.5 as a function of the incident energy. It can be observed that the elastically backscattered electron emission yield on BN is more than three times lower than on SiO_2. The energetic efficiency of electron/wall interaction can be observed on Fig.6. In order to represent a realistic case of interaction between the electrons of a plasma and a wall, R_E values have been integrated on a Lambertian distribution of incident electrons and are presented as a function of incident electron temperature (T_0, cf. Fig.7). To ease data use, R_T data have been fitted and the curve expression, parameters values and correlation coefficient can be found in Table.1. It can be observed that R_E and R_T of BN are three times lower than for SiO_2.

Table 1: Vaughan and Sombrin fitted models, parameters and correlation coefficients

Models	**Corresponding curve**	**Equations**	**Parameters**	**Correlation coefficient**
Vaughan	TEEY	$\begin{cases}\sigma = \sigma_{\max}(ve^{1-v})^k \\ v = \frac{E_0}{E_{\max}}\end{cases}$	$E_{\max} = (299 \pm 2)\,\text{eV}$ $\sigma_{\max} = 2.016 \pm 0.003$ $k = 0.563 \pm 0.007$	$R^2 = 0.99664$
Sombrin	TEEY	$\begin{cases}\sigma(E_0) = \frac{2\sigma_{\max}\left(\frac{E_0}{E_{\max}}\right)^{\alpha}}{1+\left(\frac{E_0}{E_{\max}}\right)^{2\alpha}} \\ \alpha = \frac{\ln\left(\sigma_{\max}-\sqrt{\sigma_{\max}^2-1}\right)}{\ln\left(\frac{E_I}{E_{\max}}\right)}\end{cases}$	$\sigma_{\max} = 1.995 \pm 0.004$ $E_{\max} = (293 \pm 3)\,\text{eV}$ $E_I = (37.1 \pm 0.6)\,\text{eV}$	$R^2 = 0.99591$
R_T fitting model	$R_T(T)$	$R_T(T) = a - b \cdot e^{-\frac{T}{c}}$	$a = 0.1718 \pm 0.0002$ $b = 0.0850 \pm 0.0008$ $c = 68 \pm 1$	$R^2 = 0.999\,11$

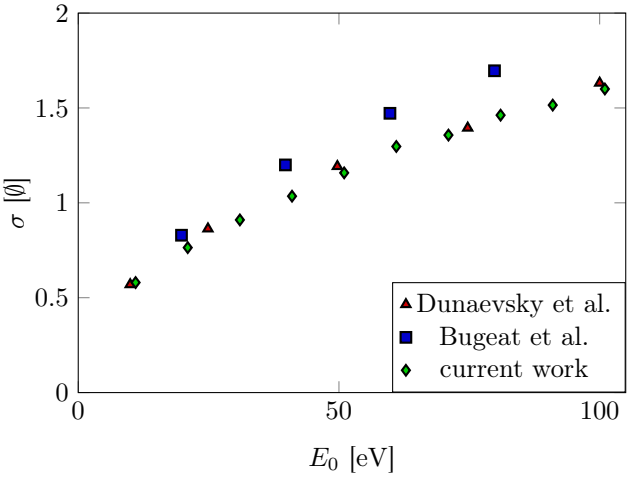

Fig. 4: Comparison between total electron emission yield of BN carried out in this study and extracted from literature.

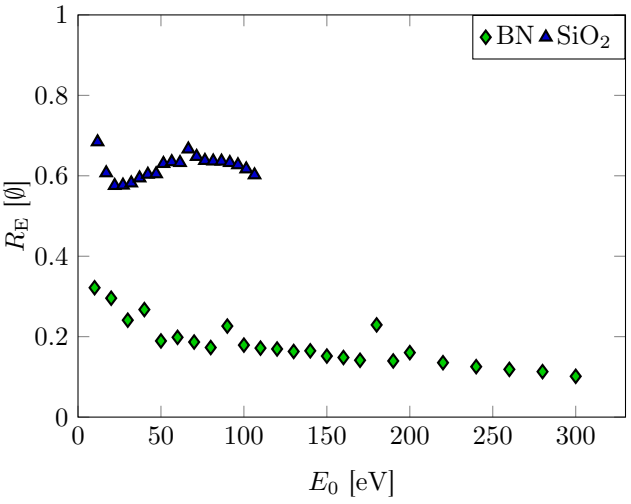

Fig. 6: Measurements of R_E as a function of incident electron energy for BN, SiO_2, Silver and Graphite samples with a monoenergetic incident electron beam of energy E_0

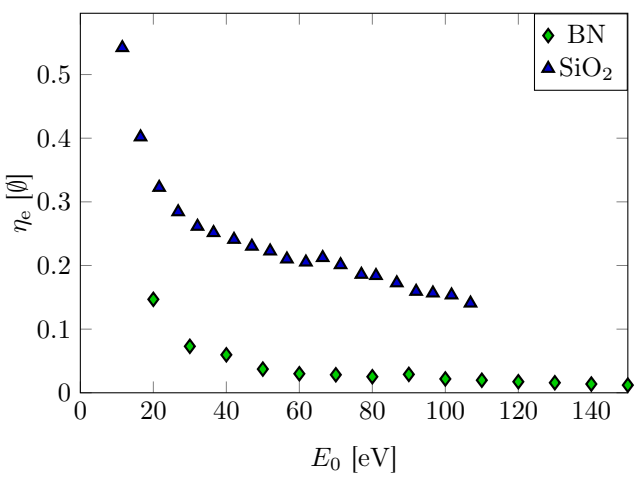

Fig. 5: Elastically backascattered electron emission yield of BN and SiO_2 samples as a function of the incident electron energy E_0 at normal incidence.

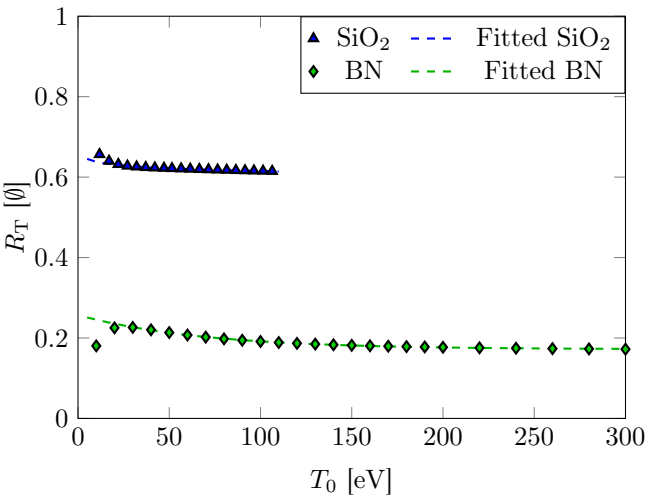

Fig. 7: Measurements of R_T as function of the incident electron temperature for Lambertian distributed incident electron beam of temperature T_0 [eV]

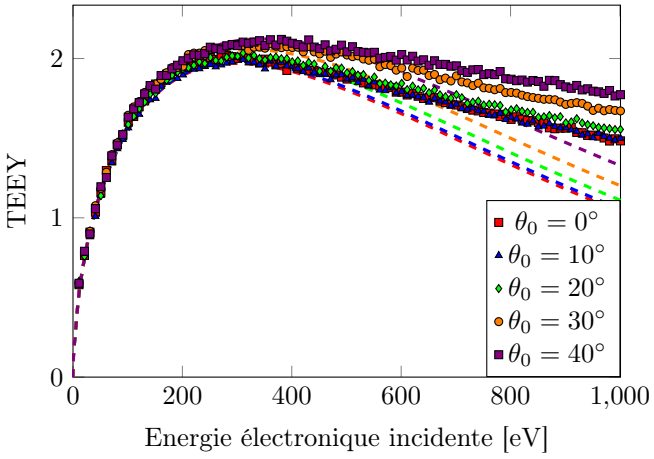

Fig. 8: Measurement of BN total electron emission yield (symbols) for an incident electron energy (E_0) between 0 eV and 1000 eV and for an incident electron angle (θ_0) between 0° and 40°. Comparison with Vaughan's fitting model (dashed lines).

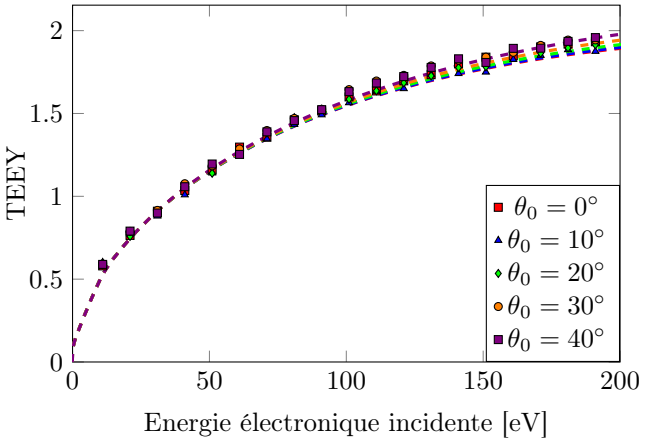

Fig. 9: Measurement of BN total electron emission yield (symbols) for an incident electron energy (E_0) between 0 eV and 200 eV and for an incident electron angle (θ_0) between 0° and 40°. Comparison with Vaughan's fitting model (dashed lines).

During the last decade much has been done to reduce wall effect on plasma behavior, for example, by testing the effect of very low emissive channel wall material (such as carbon velvet) on Hall thrusters performances [27], and changing magnetic configuration to reduce electron wall interaction [4]. Nonetheless BN and BN–SiO_2 channel walls remain an industrial standard and total electron emission yield measurements on BN (cf. Fig.3) highlights that using BN instead of BN–SiO_2 walls tends to increase electrons losses in term of number and energy at the walls. Besides, lower total electron emission yield induce a higher first energy of crossover. Thus, using ceramic materials with low total electron emission yield (like BN) could allow increasing transferred power in satellites RF components. Moreover, it is known that elastically backscattered electron emission yield plays an important role in charging phenomena on satellites solar-array and multipactor in RF components. Choosing materials with low elastically backscattered electron emission yield could allow reducing this kind of parasitic phenomena. Finally, depending on the considered issue, it could be interesting to choose material with low or high R_E (and R_T). Material with low R_E and R_T could allow absorbing the energy of an electron flux in order to stop the process. On the contrary, materials facing an intense electron flux could limit energy absorption by choosing wall high R_E (and R_T).

In this letter, the total electron emission yield, the elastically backscattered electron emission yield and the emitted electron energy distribution measurements of BN have been measured and it has been shown that it presents lower total electron emission yield, elastically backscattered electron emission yield and R_E compared to SiO_2. These new experimental data would be useful for numerous technological applications, especially in space industry. In particular it can be observed that the fitted models of total electron emission yield presented here strongly differ from the one presented by Sydorenko in his PhD. (cf. Fig.3, dotted green line) [23] and used in several articles [24, 25]. The current measurements and fits show indeed a total electron emission yield which is only two third of the one given by Sydorenko.

* * *

Mr. Villemant benefits from an Onera/Cnes PhD. fellowship. Moreover, the authors are grateful to T. Gineste to allow using its calibration values and substantial experimental data for this work. This work is supported by the CNES Research and Technology Program.

REFERENCES

[1] N. Gascon, M. Dudeck, and S. Barral. Wall material effects in stationary plasma thrusters. I. Parametric studies of an SPT-100. *Physics of Plasmas*, 10:4123, 2003.

[2] Hirokazu Tahara, Katsumi Imanaka, and Seiro Yuge. Effects of channel wall material on thrust performance and plasma characteristics of Hall-effect thrusters. *Vacuum*, 80:1216, 2006.

[3] Michael Campanell and Hongyue Wang. Influence of emitted electrons transiting between surfaces on plasma-surface interaction. *Applied Physics Letters*, 103:104104, 2013.

[4] Lou Grimaud and Stéphane Mazouffre. Conducting wall Hall thrusters in magnetic shielding and standard configurations. *Journal of Applied Physics*, 122:033305, 2017.

[5] N. Fil, M. Belhaj, J. Hillairet, and J. Puech. Multipactor threshold sensitivity to total electron emission yield in small gap waveguide structure and TEEY models accuracy. *Physics of Plasmas*, 23:123118, 2016.

[6] R. A. Kishek, Y. Y. Lau, L. K. Ang, A. Valfells, and R. M. Gilgenbach. Multipactor discharge on metals and

dielectrics: Historical review and recent theories. *Physics of Plasmas*, 5:2120, 1998.

[7] V. E. Semenov, E. I. Rakova, A. G. Sazontov, I. M. Nefedov, V. I. Pozdnyakova, I. A. Shereshevskii, D. Anderson, M Lisak, and J. Puech. Simulations of multipactor thresholds in shielded microstrip lines. *Journal of Physics D: Applied Physics*, 42:205204, 2009.

[8] K. C. Harkay. Theory and measurement of the electron cloud effect. In *Proceedings of the 1999 Particle Accelerator Conference (Cat. No.99CH36366)*, volume 1, page 123 vol.1, 1999.

[9] D. R. Grosso, P. Barone, A. Bonanno, M. Camarca, A. Oliva, F. Xu, Lab Iis, and Dep Phys. scrubbing Process of Cu Surfaces Induced by Electron Bombardment. In *Proceedings of 11th the European Particle Accelerator Conference*, 2008.

[10] D. Tskhakaya. One-dimensional plasma sheath model in front of the divertor plates. *Plasma Physics and Controlled Fusion*, 59:114001, 2017.

[11] M. Bacharis. Floating potential of large dust grains with electron emission. *Physics of Plasmas*, 21:074501, 2014.

[12] A. Autricque, N. Fedorczak, S. A. Khrapak, L. Couëdel, B. Klumov, C. Arnas, N. Ning, J.-M. Layet, and C. Grisolia. Magnetized electron emission from a small spherical dust grain in fusion related plasmas. *Physics of Plasmas*, 24:124502, 2017.

[13] L. G. Dyachkov, A. G. Khrapak, and S. A. Khrapak. Effect of electron emission on the charge and shielding of a dust grain in a plasma: A continuum theory. *Journal of Experimental and Theoretical Physics*, 106:166, 2008.

[14] M. Belhaj, J. Roupie, O. Jbara, J. Puech, N. Balcon, and D. Payan. Electron emission at very low electron impact energy: experimental and Monte-Carlo results. *arXiv preprint arXiv:1308.1301*, 2013.

[15] M Belhaj, T Tondu, V Inguimbert, and J P Chardon. A Kelvin probe based method for measuring the electron emission yield of insulators and insulated conductors subjected to electron irradiation. *Journal of Physics D: Applied Physics*, 42:105309, 2009.

[16] A. Stacey, S. Prawer, S. Rubanov, R. Ahkvlediani, Sh. Michaelson, and A. Hoffman. The effect of temperature on the secondary electron emission yield from single crystal and polycrystalline diamond surfaces. *Applied Physics Letters*, 95:262109, 2009.

[17] M. Commisso, P. Barone, A. Bonanno, R. Cimino, D. Grosso, M. Minniti, A. Oliva, P. Riccardi, and F. Xu. Angular dependence of secondary electron emission from Cu surfaces induced by electron bombardment. *Journal of Physics: Conference Series*, 100:092013, 2008.

[18] Marc Villemant, P. Sarrailh, Mohamed Belhaj, Laurent Garrigues, and Claude Boniface. Experimental investigation about Energy balance of electron emission from materials under electron impacts at low energy: application to silver, graphite and sio2. *Journal of Physics D: Applied Physics*, 2017.

[19] C. Inguimbert, J. Pierron, M. Belhaj, and J. Puech. Extrapolated Range Expression for Electrons Down to 10 eV. In *Proceedings of the 2016 Nuclear and Space Radiation Conference*, 2016.

[20] O. Kurniawan and V. K. S. Ong. Investigation of Range-energy Relationships for Low-energy Electron Beams in Silicon and Gallium Nitride. *Scanning*, 29:280, 2007.

[21] Sung Kyu Jang, Jiyoun Youn, Young Jae Song, and Sungjoo Lee. Synthesis and Characterization of Hexagonal Boron Nitride as a Gate Dielectric. *Scientific Reports*, 6:30449, 2016.

[22] J.R.M. Vaughan. A new formula for secondary emission yield. *IEEE Transactions on Electron Devices*, 36:1963, 1989.

[23] Dmytro Sydorenko. *Particle-in-cell simulations of electron dynamics in low pressure discharges with magnetic fields*. PhD thesis, University of Saskatchewan Saskatoon, 2006.

[24] Dmytro Sydorenko, Andrei Smolyakov, Igor Kaganovich, and Y Raitses. Modification of electron velocity distribution in bounded plasmas by secondary electron emission. *Plasma Science, IEEE Transactions on*, 34:815, 2006.

[25] Y Raitses, I D Kaganovich, A Khrabrov, D Sydorenko, N J Fisch, and A Smolyakov. Effect of Secondary Electron Emission on Electron Cross-Field Current in ExB Discharges. *IEEE Transactions on Plasma Science*, 39(4):995, 2011.

[26] A. Dunaevsky, Y. Raitses, and N. J. Fisch. Secondary electron emission from dielectric materials of a Hall thruster with segmented electrodes. *Physics of Plasmas*, 10:2574, 2003.

[27] S. Tsikata, A. Héron, and C. Honoré. Hall thruster microturbulence under conditions of modified electron wall emission. *Physics of Plasmas*, 24:053519, 2017.